Optical Coherence Tomography (OCT) Image Classification for Retinal Disease Using a Random Forest Classifier

Asad Wali[1], Zobia Suhail[1], Arjun Sipani[2]
[1] Department of Computer Science, Punjab University College of Information Technology (PUCIT), Lahore, Pakistan
[2] William B Travis HS, Richmond, TX, United States
*__Corresponding Author__: Asad Wali Email: asadhamid27@gmail.com

Abstract

Optical coherence tomography (OCT) is a vital imaging technique that provides detailed images of the retina and plays a crucial role in diagnosing and monitoring various retinal conditions, such as diabetic macular edema (DME), choroidal neovascularization (CNV), and DRUSEN. However, there is a need to improve the early detection and treatment of these common eye diseases. While deep learning methods have demonstrated superior accuracy in analyzing OCT images, the potential of machine learning approaches, especially concerning data volume and computational efficiency, requires further exploration. This study aimed to improve the diagnosis and management of retinal diseases using OCT images through a machine learning framework employing a random forest classifier, with a focus on comparing its efficacy against that of popular image processing filters. We propose a novel approach that uses raw image data embedding (RIDE) as input to our machine learning model. This approach uses translated image raw data as opposed to metadata-driven preprocessing algorithms. We systematically benchmark its performance against established built-in methods, such as histogram of oriented gradients (HOG), local binary patterns (LBP), and features from the opponent space for filtering (FOSF). This comparative analysis serves to assess the efficacy of our approach in relation to these widely recognized methods. The proposed method achieves higher accuracy but also optimizes the time complexity of the system. The proposed model exhibited a commendable accuracy rate of 80% in the classification of retinal diseases, surpassing the performance of various other classifiers and methods. This research represents a small step toward the creation of an accurate and efficient machine learning-based system for diagnosing and monitoring retinal diseases, ultimately contributing to improved patient outcomes and diagnostic accuracy.

Keywords: random forest classifier (RFC), support vector machine (SVM), machine learning, optical coherence tomography (OCT), diabetic macular edema (DME), choroidal neovascularization (CNV), DRUSEN, NORMAL, raw image data embedding (RIDE)

Declarations:

Ethics approval and consent to participate

All participants provided written informed consent to participate in this study. This research do not involve any other human participation, rather an online dataset is used that is publicly available and is being used by many researchers.

This study did not involve human participants and used publicly available datasets. The research adhered to ethical guidelines for the use of publicly available data, ensuring proper citation and usage according to the terms of the dataset providers.

The study was approved by the Institutional Review Board (IRB) of **Department of Computer Science, Punjab University College of Information Technology (PUCIT), Lahore, Pakistan.**

Consent for publication

Not Applicable

Availability of data and material

The datasets used and/or analyzed during the current study are publicly available at https://www.kaggle.com/datasets/paultimothymooney/kermany2018
License number: CC BY-NC-SA 4.0

Competing interests

The authors declare that they have no known competing interests or personal relationships that could have appeared to influence the work reported in this paper.

Funding

This research did not receive any specific grant from funding agencies in the public, commercial, or not-for-profit sectors.

Authors' contributions

AW contributed to the design and implementation of the research, to the analysis of the results and to the writing of the manuscript. **AP** make table and diagrams and implement some experiments. All

authors read and approved the final manuscript. **ZS** Visualization, Supervision, Project administration, Investigation, Formal analysis, Validation.

Acknowledgements

We would like to express our sincere gratitude to our supervisor, **Dr. Zobia Suhail**, for her invaluable guidance, support, and encouragement throughout the course of this research. Her expertise and insights have been instrumental in the successful completion of this study.

Introduction:

Optical coherence tomography (OCT) has emerged as a rapidly advancing medical imaging technique in recent years. It has the capability to capture various characteristics of biological tissues, including blood flow, polarization status, structural data, elastic parameters, and molecular content [1]. The retina, the only light sensor in the human eye, transforms light information into bioelectric signals and transmits them to the brain via the optic nerve [2]. This process is crucial for human vision. Retinal diseases such as age-related macular degeneration (AMD), diabetic macular edema (DME) and choroidal neovascularization (CNV) are major contributors to vision loss and permanent blindness globally [3]. A recent survey revealed that approximately 90% of vision loss can be prevented and treated through precise retinal screening and timely intervention in the early stages. Therefore, accurate diagnosis of retinal diseases is paramount in clinical settings.

Optical coherence tomography (OCT) is a noninvasive imaging technology that generates high-resolution cross-sectional images of biological tissue. By analyzing the light reflected and backscattered from retinal tissue, OCT enables visualization of the structures of various retinal layers. In particular, spectral domain OCT (SD-OCT) [4] has gained prominence in ophthalmology due to its superior image quality, allowing for the early detection of treatable conditions before the onset of visual symptoms and irreversible vision loss. Despite its benefits, manually interpreting and diagnosing retinal diseases from the vast amount of OCT images can be laborious, time intensive, and subjective.

Advances in biomedical imaging, sensing technologies, high-performance computing, and artificial intelligence algorithms have paved the way for intelligent disease diagnosis. Various automated diagnostic methods have been developed to identify retinal diseases using OCT imaging. Traditional approaches rely on machine learning models to classify OCT images by extracting handcrafted features through well-designed descriptors and feeding them into a classifier for classification. In contrast, deep neural networks have revolutionized this field by learning to extract features directly from raw data at different levels. Deep convolutional neural networks have been particularly successful in retinal OCT image classification due to their ability to capture translation invariance and local features effectively.

OCT has diverse clinical applications across various medical fields, including ophthalmology [5,6], cardiology [7,8], endoscopy [9,10], and dermatology and oncology [11,12]. In developmental biology, OCT has been instrumental in characterizing the morphological and functional development of organs such as the eyes [13], brain [14], limbs [15], reproductive organs [16], and heart [17,18]. This versatile imaging technology has significantly contributed to advancing our understanding and diagnostic capabilities in a wide range of medical disciplines, benefiting both clinical practice and research.

In the context of ophthalmology, OCT has demonstrated promising outcomes in diagnosing retinal diseases by providing high-resolution cross-sectional images of the eye's soft tissues, particularly the retina. It enables noninvasive examination and evaluation of the retina, aiding in the detection and assessment of various eye conditions, such as diabetic macular edema (DME), glaucoma, and choroidal neovascularization (CNV) [19,20]. Morphological features such as drusen, macular holes, and blood vessel characteristics can be readily identified on

OCT images, serving as important disease indicators. Consequently, OCT imaging is essential for conducting comprehensive studies on changes in retinal structures, with techniques emphasizing the consistency of OCT layers to ensure accurate results [21].

In recent years, OCT technology has experienced significant progress fueled by advancements in light sources, detection systems, and signal-processing methods. The combination of adaptive optics with OCT has further expanded possibilities by correcting aberrations, leading to enhanced clarity in visualizing the cellular structures of the retina.

This study focused on exploring the latest advancements and uses of optical coherence tomography (OCT), particularly in enhancing our knowledge of retinal diseases and aiding clinical interventions. Machine learning plays a crucial role in the analysis of OCT images, as it can effectively identify and categorize subtle pathological characteristics, often outperforming manual analysis in terms of speed and precision. Furthermore, sophisticated algorithms can leverage extensive datasets of OCT images to facilitate the early identification of conditions such as macular degeneration and diabetic retinopathy, which is essential for prompt treatment. One distinctive aspect of this study is the novel approach employed for preprocessing OCT data. In this methodology, we use raw image data embedding (RIDE) as a feature and apply it to a random forest classifier. The effectiveness of this method is then compared to that of existing approaches to determine its superiority in terms of diagnostic accuracy. While the broader context explores the potential of machine learning and artificial intelligence in automating OCT image classification and analysis, our focus lies in the innovative preprocessing step and its impact on improving diagnostic outcomes. Addressing challenges such as limited annotated datasets, domain adaptation, and the interpretability of complex models remains crucial, and our study contributes by introducing and evaluating a unique preprocessing technique within the realm of OCT research.

Literature Review:

Optical coherence tomography (OCT) has become a valuable imaging tool in medical diagnostics, especially in ophthalmology, offering detailed cross-sectional images of biological tissues. The increasing availability of OCT data has spurred interest in developing efficient methods for OCT image classification to improve diagnostic accuracy and streamline clinical decision-making. Classifying OCT images presents challenges due to intricate structural patterns and subtle tissue variations. Researchers have explored various approaches, including traditional machine learning methods, deep learning architectures, and hybrid models, to effectively distinguish between normal and pathological conditions. Initially, feature extraction techniques were pivotal in extracting relevant information from OCT images for training classifiers. In recent years, deep learning methods, particularly convolutional neural networks (CNNs), have gained traction for their ability to automatically learn hierarchical representations from raw OCT data.

Wali, Asad et al. [22] conducted experiments on an OCT dataset, exploring various built-in feature extraction methods across three distinct machine learning classifiers. Their study aimed to identify the most effective combination of feature extraction methods and machine learning classifiers for accurately categorizing OCT images. Researchers have likely tested methods that can effectively capture relevant information, such as texture, shape, or other distinctive features, from OCT images. The researchers found that when the HOG feature extraction method was paired with the support vector machine (SVM) classifier, it yielded

superior performance compared to other combinations. SVM is a powerful algorithm for classification tasks and is known for its ability to find the optimal hyperplane that best separates different classes in a high-dimensional feature space. This suggests that the combination of HOG features and SVM classification was particularly well suited for the characteristics of the OCT dataset, resulting in 78.8% accuracy and reliable categorization of the images.

Srinivasan et al. [23] utilized machine learning techniques for diagnosing and analyzing AMD and DME diseases using OCT images. The authors extracted histogram of oriented gradients (HOG) features from OCT images and implemented support vector machines (SVMs) for classification and recognition.

The study by Schmidt-Erfurth et al. [24] compared unsupervised and supervised learning methods for binary classification in patients with macular degeneration and diabetic retinopathy using a deep learning approach on a dataset of approximately 20,000 images. The research achieved a high accuracy of up to 97% in distinguishing between healthy individuals and those with AMD. The team employed a deep denoising autoencoder (DDAE) trained on healthy samples to identify features that differentiate normal tissue from anomalies in SD-OCT scans. They also utilized support vector machines (SVMs) to model normal probability distributions and a clustering technique to detect inconsistencies in the data. The identified categories were then evaluated by retinal experts, with some matching known retinal structures and others representing novel anomalies not previously associated with known structures. The study revealed that these novel categories were also linked to disease, highlighting the potential of these methods in disease detection and classification.

Lee et al. [25] developed a 21-layer convolutional neural network (CNN) for the purpose of ranking AMD disease, achieving a notable 93% accuracy in binary classification between AMD and normal cases. Kermanni et al. [26] presented a CNN solution utilizing the Inception V3 model and employing transfer learning, resulting in an impressive 96.6% accuracy on a dataset comprising approximately 84,000 samples categorized into drusen, CNV, and DME classes. Huang and team [27] introduced a CNN-based classification approach for distinguishing normal retina, CNV, DME, or drusen, achieving an accuracy rate of 89.9%. Another study by Huang et al. [28] proposed a method based on the Inception V3 model. Tsuji et al. [29] demonstrated high accuracies of 99.6% and 99.8% using the capsule network and InceptionV3, respectively. Prabhakaran introduced the OctNET model, which achieved an impressive 99.69% accuracy on the Kermany database, featuring a relatively lightweight architecture suitable for fast computations. In a separate study, G Latha and P Aruna Priya [30] concentrated on assessing the efficacy of various machine learning classifiers in detecting glaucoma in retinal images. Their approach integrated Gabor transforms and efficient computational classification techniques, utilizing support vector machine (SVM), neural network (NN), and adaptive neurofuzzy inference system (ANFIS) classifiers to evaluate the performance of the glaucoma retinal image classification system.

Roychowdhury et al. [31] developed a method to localize cysts in OCT images of patients with diabetic macular edema (DME). The approach involved identifying six subretinal layers in each image through an iterative high-pass filtering technique. Subsequently, dark regions were identified as potential cystoid regions. To estimate the area of these regions, features such as the solidity, mean, and maximum pixel value of the negative OCT image were analyzed for each candidate cystoid region. The algorithm successfully delineated the boundaries of contiguous cysts, enabling the breakdown of large cysts. The system

demonstrated the ability to detect cystoid areas with a mean error of 4.6% and a standard deviation of 6.6% based on 120 OCT images from 25 DME patients. It achieved a sensitivity of 100% and specificity of 75% in distinguishing images with cysts from those without. Moreover, there was a 90% correlation between the manually segmented area and the cystoid area identified by the algorithm. The algorithm accurately located cysts in the inner plexiform layer with 88% accuracy, in the inner nuclear layer with 86% accuracy, and in the outer nuclear region with 80% accuracy.

Zhou [32] presented an automated system for diabetic retinopathy (DR) detection using a deep learning approach comprising two main stages: image preprocessing and deep learning classification. In the preprocessing stage, morphological operations, adaptive histogram equalization, and vessel segmentation techniques were employed to enhance image quality and reduce noise. For classification, the study utilized a pretrained EfficientNet-B4 model that was fine-tuned on a DR fundus image dataset to classify images into five levels of DR severity. Data augmentation methods such as random rotation, flipping, and cropping were implemented to improve the model's generalizability. The system was evaluated on two public datasets and achieved high accuracy and outperformed existing state-of-the-art techniques in diabetic retinopathy detection.

Jian Li [33] developed an advanced deep learning system for the detection and classification of diabetic retinopathy (DR) involving four key stages: initial image processing, image enhancement, subtraction, and classification. The process commenced with enhancing retinal image quality through morphological operations and contrast-limited adaptive histogram equalization (CLAHE), followed by binary thresholding for segmentation. The image enhancement phase utilized a dual attention mechanism to enhance image quality by focusing on both channel and spatial relationships. Feature extraction was performed using the EfficientNet-B4 model, which was fine-tuned on a DR fundus imaging dataset. Classification was carried out using a multiclass SVM classifier to categorize images into five severity levels of DR. The system's effectiveness was evaluated on two public datasets, achieving high accuracy and surpassing existing state-of-the-art methods, highlighting its potential as a valuable tool for diagnosing and classifying diabetic retinopathy. H. Fu [34] developed a deep learning method for automatically diagnosing diabetic retinopathy (DR) using fundus images. The method achieved an impressive accuracy of 92.9%, a sensitivity of 93.5%, and a specificity of 92.5% on the test data. It demonstrated high precision, recall, and F1 scores, indicating its ability to accurately identify DR with minimal false positives. Comparative analyses with experts showed the system's superior accuracy, highlighting the potential of deep learning in DR diagnosis.

S. W. Ting et al. [35] provided a comprehensive review of artificial intelligence and deep learning advancements and applications in ophthalmology. This review likely covers the use of deep learning algorithms for tasks such as image analysis, disease detection, classification, and treatment planning for various ocular diseases. The potential impact of AI on improving diagnostic accuracy, patient outcomes, and healthcare delivery in ophthalmology should also be discussed. R. Gargeya and T. Leng [36] presented a study on a deep learning-based system for the automated identification of diabetic retinopathy. The study likely includes details on the dataset, model architecture, training procedures, and performance evaluation metrics. The clinical implications of using automated systems for DR screening, including their benefits in early detection and disease management, are also discussed. Hwang D.K. et al. [37] proposed a method based on the Inception V3 model with preprocessed images, achieving 96.9% accuracy. Tasnim et al. [38] conducted research on utilizing deep learning techniques

for analyzing retinal OCT images. Among the models explored, MobileNetV2 achieved an accuracy of 99.17% when tested on the Kermany dataset, which consists of 84,484 samples categorized into four groups.

The objective of this study was to address the current research gap concerning the application of machine learning classification techniques to OCT data. Our methodology emphasizes the use of actual or translated image pixels rather than depending solely on pixel metadata. We have chosen to implement a random forest classifier algorithm to extract meaningful insights from OCT datasets.

OCT Dataset

In this research, the OCT dataset provided by Kermany et al. [26] on Kaggle was utilized. The dataset contains a significant number of 84,484 images. Due to hardware constraints, a subset of 4,000 images was randomly chosen from the training dataset. This selection ensured that each class was represented, with 1,000 images per class included in the subset. This approach aimed to create a manageable and diverse sample for the investigation while balancing dataset size with computational limitations, thus enabling the feasibility of the experimental analysis.

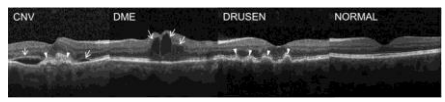

Figure 1: Optical coherence tomography images in the OCT dataset.

Proposed Method

This study presents a solution for disease classification based on OCT images. We emphasize that these solutions must be both effective and accurate. Therefore, this paper presents a highly optimized solution using a RFC model. Machine learning plays an important role in addressing various real-world problems. Features were extracted from the OCT images in the RIDE (raw image data embedding) form, and these features were subsequently classified as normal or diseased via random forest classification. The main aim of this study is to maximize task efficiency while minimizing the use of computing resources. We propose solutions using public databases to ensure that our work is comparable and reproducible.

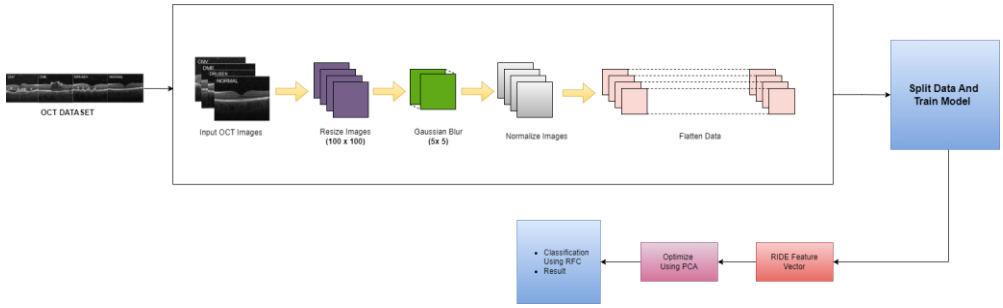

Figure 2: Flow diagram of the proposed method. Features are extracted by the RIDE method, and PCA is applied to the feature vector for optimization and final classification.

Data Preprocessing

For preprocessing, the OCT dataset is imported from the directory. Each image is read from the corresponding folder of the dataset and then resized to a square shape with dimensions of 100 × 100 pixels. After resizing, Gaussian blur is applied to remove noise from the images. Upon successful resizing and noise removal, each image, along with its corresponding class label ('CNV', 'DME', 'DRUSEN', or 'NORMAL'), is appended to the training data list.

Data normalization

The pixel values are normalized by dividing each pixel by 255. This is a common preprocessing step for image data, as it scales the pixel values to a range of 0 to 1, which can help the model learn more efficiently. In this study, the data were split into training and testing sets.

Flatten Data

The image data were flattened before being fed into the classifiers. This was achieved using the reshape function provided by the NumPy library. The reshape function allows us to change the shape of an array while preserving its data. By reshaping the multidimensional image arrays into one-dimensional arrays, we transformed each image into a single row of pixel values. After flattening, each image was represented as a one-dimensional array. These flattened arrays served as the input data for our machine learning classifiers.

Model training

The training-test split function randomly splits the data into training and testing sets. The default split was 80% for training and 20% for testing. The arrays are then passed as input to the function, which returns the training data and test data. The training dataset is used to train the machine learning model, while the testing dataset is used to evaluate the model's performance on unseen data.

Random forest classifier

The random forest classifier is a supervised machine learning algorithm used for classification. It is an integrated learning process that creates multiple decision trees and combines their results to make predictions. The RF algorithm has two stages: (i) RF generation and (ii) RF prediction based on the RF classifier created in the first stage. The main idea behind the random forest approach is to create multiple decision trees, each training on a different set of training data and using different features. To build each decision tree, the algorithm randomly selects a set of training data and a set of features. It then uses these selected training data and features to create a decision tree. The algorithm considers the results of each decision tree in the forest when making predictions. For classification tasks, each tree in the forest predicts a list of input classes, and the final prediction is based on the majority vote across all the trees' predictions.

Prediction

The presented paper uses a random forest classifier (RFC) imported from the sklearn module, a popular ensemble learning method for classification tasks. The RFC object was instantiated with two parameters: (i) maximum depth and (ii) random state. In this research, the maximum depth value was set to 200, and the random state was set to 200. The max depth parameter sets the maximum depth of each decision tree in the forest, ensuring that each tree can reach up to 200 layers. This can result in more complex trees, potentially capturing intricate relationships in the data, although a very high maximum depth may increase the risk of overfitting. The random state parameter sets the random seed used by the RFC, ensuring consistent results in each run with the same random state value. This deterministic behavior allows us to reproduce the same results consistently, aiding in debugging, comparison, and reproducibility of the results. To train the model, the 'fit' method of the random forest classifier object is called with the training data. Subsequently, the 'predict' method of the classifier is used to predict the labels of the test data. The predictions are stored as variables, the accuracy is calculated, and both a confusion matrix and a distribution map are generated.

Results and Discussion:

This paper introduces a unique preprocessing method combined with a random forest classifier, achieving an 80% accuracy in distinguishing between normal and diseased OCT images.

Comparison with other models and classifiers

This paper also conducts an in-depth comparative analysis of the proposed RIDE method against a range of models and classifiers for retinal disease classification. This study offers a detailed comparison across various models for retinal disease distribution, emphasizing both time efficiency and accuracy tailored to the specific requirements of each method. We employed three distinct feature extraction techniques in this research: histogram of oriented gradients (HOG), local binary pattern (LBP), and Fourier transform of spectral features (FOSF). Additionally, the study incorporates three widely used classification approaches: random forest classification (RFC), support vector machine (SVM), and K-nearest neighbor (KNN).

Raw image data embedding (RIDE)

Raw image data embedding (RIDE) is a novel feature extraction method for image analysis and classification. This technique utilizes a linearized subset of an image's pixels as input for machine learning classifiers. In this study, RIDE was applied to a dataset in combination with three different classifiers: random forest, support vector machine (SVM), and K-nearest neighbors (KNN). By embedding raw pixel data, RIDE provides a distinctive approach to feature representation, aiming to capitalize on the inherent details present in raw images and effectively integrate them with the unique classification capabilities of random forest, SVM, and KNN. This integration of RIDE with these classifiers facilitates an exhaustive examination of the dataset, endeavoring to maximize efficiency in image analysis and classification tasks. The performance of this approach, evaluated through key metrics such as accuracy, precision, recall, and F1 score, offers insight into the efficacy of RIDE when paired with each classifier. This analysis illuminates the potential for a synergistic relationship between feature extraction techniques and classification methods in the realm of image processing.

Labels	Precision	Recall	F1-Score	Support
CNV	0.80	0.80	0.80	267
DME	0.79	0.85	0.82	257
DRUSEN	0.80	0.81	0.80	241
NORMAL	0.80	0.80	0.80	235

Table 1: Classification Report of RFC

Labels	Precision	Recall	F1-Score	Support
CNV	0.57	0.65	0.60	267
DME	0.60	0.66	0.63	257
DRUSEN	0.46	0.51	0.48	241
NORMAL	0.54	0.34	0.41	235

Table 2: Classification Report of KNN

Labels	Precision	Recall	F1-Score	Support
CNV	0.70	0.67	0.68	267
DME	0.65	0.68	0.67	257
DRUSEN	0.53	0.46	0.49	241
NORMAL	0.48	0.55	0.51	235

Table 3: Classification Report of SVM

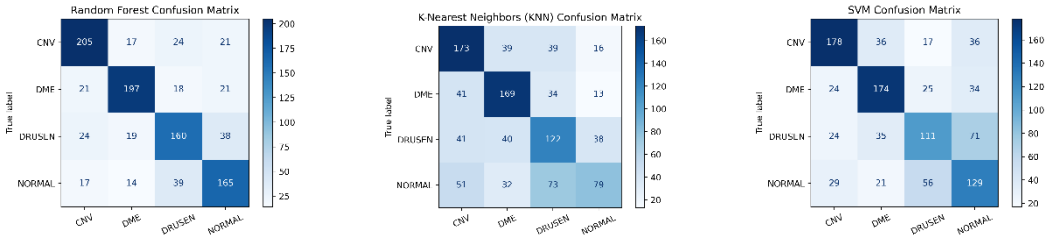

Figure 3: Confusion matrix of RFC, KNN and SVM.

Histogram of Oriented Gradients (HOGs)

The histogram of oriented gradients (HOG) is a feature descriptor extensively used in computer vision and image processing for object detection tasks. It operates by segmenting an image into smaller, overlapping sections, calculating the gradients in each section, and then categorizing these gradient orientations into histograms. This process generates feature vectors that effectively encapsulate the local intensity gradients, offering a robust representation of the shapes and structures of objects. In our study, we employed the HOG feature descriptor for the classification of OCT images, leveraging its renowned capabilities in computer vision and image processing. We applied the HOG algorithm to our dataset, which involved breaking down images into small, overlapping sections, computing the local intensity gradients, and then generating histograms that characterize the gradient orientations.

To assess the effectiveness of HOG features in object recognition, we utilized three distinct classifiers: random forest, support vector machine (SVM), and K-nearest neighbors (KNN). Our experimental approach included a meticulous division of the dataset into training and test sets, with each classifier configured appropriately. The results were comprehensively analyzed using standard evaluation metrics such as accuracy, precision, recall, and F1-score. This analysis aimed to elucidate the performance of each classifier in accurately distinguishing between different object classes, thereby highlighting the potential of HOG features in object detection and classification [22].

Labels	Precision	Recall	F1-Score	Support
CNV	0.69	0.80	0.74	259
DME	0.71	0.64	0.68	242
DRUSEN	0.65	0.65	0.65	249
NORMAL	0.72	0.68	0.70	250

Table 4: Classification Report of RFC [22]

Labels	Precision	Recall	F1-Score	Support
CNV	0.73	0.75	0.74	259
DME	0.77	0.62	0.69	242
DRUSEN	0.54	0.70	0.61	249
NORMAL	0.66	0.58	0.61	250

Table 5: Classification Report of KNN [22]

Labels	Precision	Recall	F1-Score	Support
CNV	0.76	0.85	0.80	259
DME	0.81	0.68	0.74	242
DRUSEN	0.68	0.69	0.68	249
NORMAL	0.73	0.75	0.74	250

Table 6: Classification Report of SVM [22]

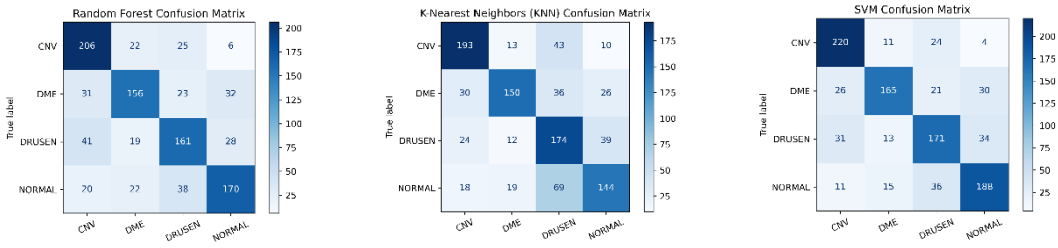

Figure 4: Confusion matrix of RFC, KNN and SVM [22]

Local Binary Pattern (LBP)

The local binary pattern (LBP) is a texture descriptor widely utilized for texture analysis and classification in image processing. It functions by comparing a central pixel's intensity with that of its surrounding pixels, encoding these relational intensities into binary patterns. These patterns are subsequently converted into histograms, effectively encapsulating the texture features of the image. LBP is particularly adept at identifying textural patterns such as edges, corners, and diverse texture variations. In our study, we applied the LBP method to our dataset and used three different classifiers for evaluation: random forest (RFC), support vector machine (SVM), and K-nearest neighbors (KNN). The goal was to determine the effectiveness of LBP, in combination with these classifiers, in differentiating various textures within the dataset, thereby offering valuable insights into its applicability for texture-centric image classification tasks.

To gauge the efficacy of the Local Binary Pattern (LBP) when used alongside the Random Forest (RFC), Support Vector Machine (SVM), and K-Nearest Neighbors (KNN) classifiers, our evaluation focused on key metrics such as accuracy, recall, precision, and the F1 score. These metrics collectively serve as critical indicators of the classifiers' proficiency in accurately detecting and classifying different textures present in the images. Accuracy indicates the overall correctness of the classifications made, recall measures the ability of the classifiers to correctly identify relevant examples of each texture class, precision assesses the exactness of the classifiers in correctly labeled instances of a specific class, and the F1 score provides a harmonized evaluation, considering both precision and recall. These performance indicators present a holistic view of the effectiveness of LBP, in combination with RFC, SVM, and KNN, in precisely classifying textures within our dataset. This analysis thereby contributes significant insights to the broader domain of texture-based image analysis [22].

Labels	Precision	Recall	F1-Score	Support
CNV	0.60	0.52	0.56	255
DME	0.54	0.57	0.56	249
DRUSEN	0.35	0.43	0.39	232
NORMAL	0.37	0.33	0.35	264

Table 7: Classification Report of RFC [22]

Labels	Precision	Recall	F1-Score	Support
CNV	0.33	0.75	0.74	255
DME	0.26	0.62	0.69	249
DRUSEN	1.00	0.03	0.06	232
NORMAL	0.00	0.00	0.00	264

Table 8: Classification Report of KNN [22]

Labels	Precision	Recall	F1-Score	Support
CNV	0.74	0.54	0.62	255
DME	0.70	0.57	0.63	249
DRUSEN	0.46	0.56	0.51	232
NORMAL	0.46	0.57	0.51	264

Table 9: Classification Report of SVM [22]

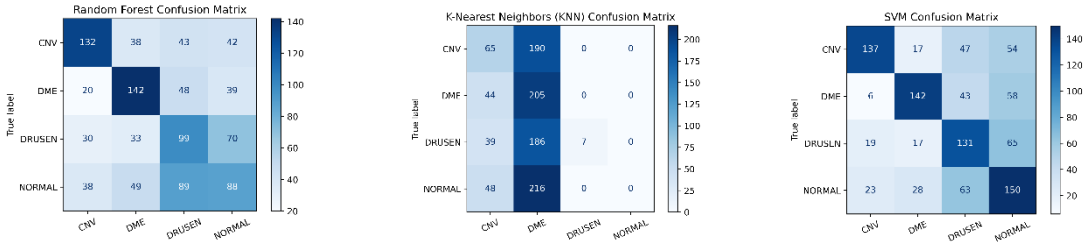

Figure 5: Confusion matrix of RFC, KNN and SVM [22]

Fourier Transform of Spectral Features (FOSF)

Fourier transform of spectral features (FOSF) is a method that employs the Fourier transform to derive spectral features from signals or images. In image processing, the FOSF translates the spatial details of an image into the frequency domain, revealing its frequency components. This conversion is pivotal in various tasks, including image compression, filtering, and feature extraction. FOSF is especially useful in fields where analyzing an image's frequency content is essential, such as in medical or satellite image analysis. To examine its effectiveness, we applied FOSF to our dataset and used three classifiers for assessment: random forest (RFC), support vector machine (SVM), and K-nearest neighbors (KNN). This technique is particularly advantageous in situations where discerning an image's frequency details is crucial, for instance, in medical imaging or satellite imagery analysis.

The next phase of our study focused on evaluating how FOSF, combined with these classifiers, performs in image processing tasks such as classification and object detection. We assessed the performance using key metrics such as accuracy, recall, precision, and F1 score. This comprehensive analysis was aimed at determining the proficiency of FOSF, in conjunction with random forest, SVM, and KNN, in accurately differentiating various patterns and structures within our dataset. The results provided a nuanced understanding of the capabilities of FOSF when integrated with different classification methods, offering valuable insights into its potential applications in the field of image analysis [22].

Labels	Precision	Recall	F1-Score	Support
CNV	0.56	0.61	0.58	235
DME	0.52	0.51	0.52	247
DRUSEN	0.48	0.44	0.46	277
NORMAL	0.42	0.43	0.42	241

Table 10: Classification Report of RFC [22]

Labels	Precision	Recall	F1-Score	Support
CNV	0.38	0.54	0.45	235
DME	0.37	0.41	0.39	247
DRUSEN	0.39	0.30	0.34	277
NORMAL	0.39	0.29	0.33	241

Table 11: Classification Report of KNN [22]

Labels	Precision	Recall	F1-Score	Support
CNV	0.36	0.51	0.42	235
DME	0.37	0.32	0.34	247
DRUSEN	0.31	0.06	0.11	277
NORMAL	0.37	0.59	0.45	241

Table 12: Classification Report of SVM [22]

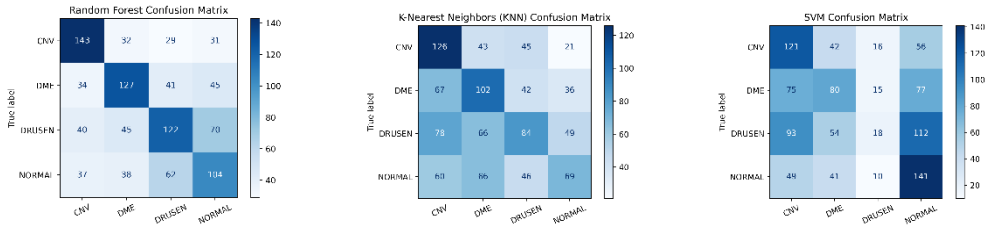

Figure 6: Confusion matrix of RFC, KNN and SVM [22]

In addition to these feature extraction techniques, a baseline comparison was established by utilizing RIDE as the input for each of the three classifiers. This approach aimed to evaluate the inherent performance of the classifiers.

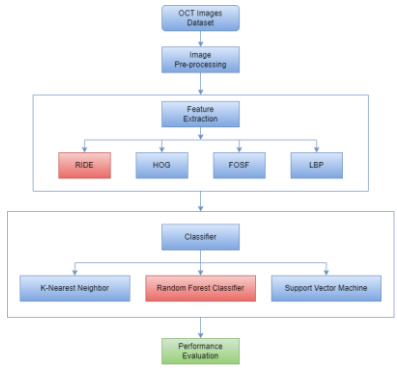

Figure 7: Proposed methodology with existing methods.

The results of this study provide fascinating insights into the relative effectiveness of the explored methods. Universally, the random forest classifier (RFC) outperformed the support vector machine (SVM) and K-nearest neighbors (KNN) classifiers not only in accuracy but also in computational efficiency. Most strikingly, the combination of raw image data embedding (RIDE) with the random forest classifier achieved the highest accuracy and required the least computational time among all the combinations tested. This indicates that RIDE-RFC pairing could be an especially powerful and dependable approach for detecting retinal diseases.

Methods	**No. of Attributes**	**Accuracy (RFC)**	**Accuracy (KNN)**	**Accuracy (SVM)**
RIDE	10,000	**80%**	54%	59%
HOG	10,000	69%	66%	74%
FOSF	10,000	49%	38%	36%
LBP	10,000	46%	27%	56%

Table 13: ACCURACY of the proposed methods on the OCT dataset

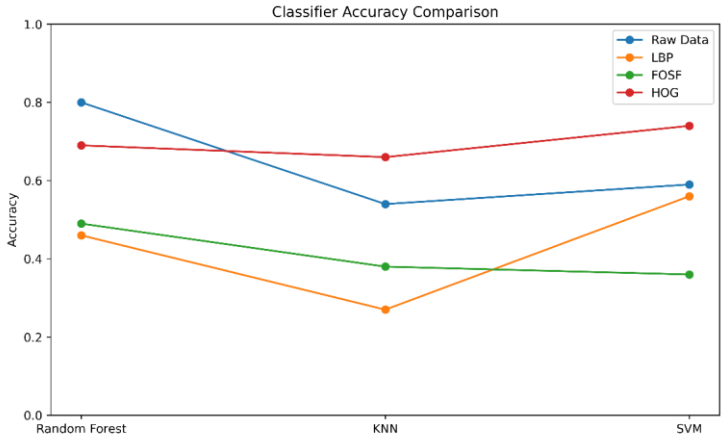

Figure 8: Accuracy comparison of different models and classifiers

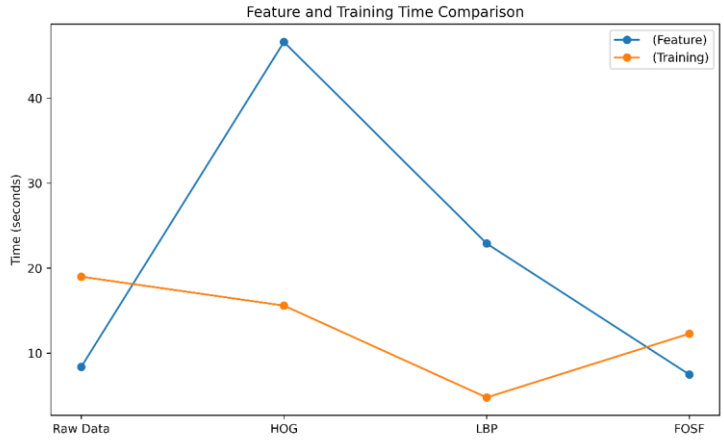

Figure 9: Time comparison of different models

This paper goes beyond merely comparing different feature extraction techniques and classifiers for retinal disease detection; it also emphasizes the importance of judiciously choosing the most effective combination of filters and classifiers to achieve enhanced accuracy. The results underscore the notable benefits of integrating raw image data embedding (RIDE) with the random forest classifier. This provides critical insights for future studies and practical implementations in medical image analysis, highlighting a promising direction for advancements in this field.

Conclusion:

In conclusion, this paper proposed a precise and efficient system for OCT image analysis and classification utilizing RIDE as a preprocessing tool for a random forest classifier. In addition, a detailed comparison of various combinations of filters and classifiers used in

retinal disease classification is presented. The proposed RIDE filter, along with the RFC, enhances the diagnosis and management of retinal diseases by offering swift and objective OCT image processing. However, there is a need for further research to understand the application of this system to larger datasets and its clinical utility. Future investigations could focus on several critical areas. First, expanding the dataset in terms of size and diversity is essential to strengthen the model's ability to identify complex patterns in retinal images. Careful adjustment of the random forest classifier's hyperparameters, such as tree depth and the number of trees in the forest, offers the potential to refine the model's learning process.

Additionally, optical coherence tomography (OCT) images allow for an in-depth analysis of structural features present in the tissues imaged. Investigating detailed aspects of anatomical structures, such as the thickness of layers, vessel density, and unique markers within retinal tissues, could unveil sophisticated structure-based features pivotal for increasing diagnostic accuracy. Future research endeavors should aim to increase the precision of OCT image analysis systems, thereby significantly contributing to their practical application in clinical settings.

References

[1] D. Huang, E. Swanson, C. Lin, J. Schuman, W. Stinson, W. Chang, M. Hee, T. Flotte, K. Gregory, C. Puliafito, and J. Fujimoto: Optical coherence tomography. Science, 254, 1178–1181 (1991) DOI: 10.1126/science.1957169

[2] Lin, Y.; Xiang, X.; Chen, T.; Mao, G.; Deng, L.; Zeng, L.; Zhang, J. In vivo monitoring the dynamic process of acute retinal hemorrhage and repair in zebrafish with spectral-domain optical coherence tomography. J. Biophotonics 2019, 12, e201900235

[3] Lim, L.S.; Mitchell, P.; Seddon, J.M.; Holz, F.G.; Wong, T.Y. Age-related macular degeneration. Lancet 2012, 379, 1728–1738.

[4] Wojtkowski M et al. Ophthalmic imaging by spectral optical coherence tomography. Am J Ophthalmol. 2004 Sep;138(3):412-9

[5] B. Potsaid, I. Gorczynska, V. J. Srinivasan, Y. Chen, J. Jiang, A. Cable, and J. G. Fujimoto: Ultrahigh speed spectral/Fourier domain OCT ophthalmic imaging at 70,000 to 312,500 axial scans per second. Opt Express, 16, 15149–15169 (2008) DOI: 10.1364/OE.16.015149

[6] M. E. van Velthoven, D. J. Faber, F. D. Verbraak, T. G. van Leeuwen, and M. D. de Smet: Recent developments in optical coherence tomography for imaging the retina. Prog Retin Eye Res, 26, 57–77 (2007) DOI: 10.1016/j.preteyeres.2006.10.002

[7] S. A. Boppart, G. J. Tearney, B. E. Bouma, J. F. Southern, M. E. Brezinski, and J. G. Fujimoto: Noninvasive assessment of the developing Xenopus cardiovascular system using optical coherence tomography. Proceedings of the National Academy of Sciences 94, 4256–4261 (1997) DOI: 10.1073/pnas.94.9.4256

[8] M. J. Suter, S. K. Nadkarni, G. Weisz, A. Tanaka, F. A. Jaffer, B. E. Bouma, and G. J. Tearney: Intravascular optical imaging technology for investigating the coronary artery. JACC Cardiovasc Imaging, 4, 1022– 1039 (2011) DOI: 10.1016/j.jcmg.2011.03.020

[9] G. Tearney, M. Brezinski, J. Fujimoto, N. Weissman, S. Boppart, B. Bouma, and J. Southern: Scanning single-mode fiber optic catheter–endoscope for optical coherence tomography. Opt Lett, 21, 543–545 (1996) DOI: 10.1364/OL.21.000543

[10] G. J. Tearney, M. E. Brezinski, B. E. Bouma, S. A. Boppart, C. Pitris, J. F. Southern, and J. G. Fujimoto: In vivo endoscopic optical biopsy with optical coherence tomography. Science, 276, 2037–2039 (1997) DOI: 10.1126/science.276.5321.2037

[11] T. Gambichler, G. Moussa, M. Sand, D. Sand, P. Altmeyer, and K. Hoffmann: Applications of optical coherence tomography in dermatology. J Dermatol Sci, 40, 85–94 (2005) DOI: 10.1016/j.jdermsci.2005.07.006

[12] J. Schmitt, M. Yadlowsky, and R. Bonner: Subsurface imaging of living skin with optical coherence microscopy. Dermatology, 191, 93–98 (1995) DOI: 10.1159/000246523

[13] K. D. Rao, Y. Verma, H. Patel, and P. Gupta: Noninvasive ophthalmic imaging of adult zebrafish eye using optical coherence tomography. Curr Sci, 90, 1506 (2006)

[14] L. Kagemann, H. Ishikawa, J. Zou, P. Charukamnoetkanok, G. Wollstein, K. A. Townsend, M. L. Gabriele, N. Bahary, X. Wei, J. G. Fujimoto, and others: Repeated, noninvasive, high resolution spectral domain optical coherence tomography imaging of zebrafish embryos. Mol Vis, 14, 2157–2170 (2008)

[15] S. H. Syed, K. V. Larin, M. E. Dickinson, and I. V. Larina: Optical coherence tomography for high-resolution imaging of mouse development in utero. J Biomed

Opt, 16, 46004–46004 (2011) DOI: 10.1117/1.3560300
[16] J. C. Burton, S. Wang, C. A. Stewart, R. R. Behringer, and I. V. Larina: High-resolution three-dimensional in vivo imaging of mouse oviduct using optical coherence tomography. Biomed Opt Express, 6, 2713–2723 (2015) DOI: 10.1364/BOE.6.002713
[17] A. Alex, A. Li, X. Zeng, R. E. Tate, M. L. McKee, D. E. Capen, Z. Zhang, R. E. Tanzi, and C. Zhou: A circadian clock gene, Cry, affects heart morphogenesis and function in Drosophila as revealed by optical coherence microscopy. PLoS One, 10, e0137236 (2015) DOI: 10.1371/journal.pone.0137236
[18] M. Jenkins, D. Adler, M. Gargesha, R. Huber, F. Rothenberg, J. Belding, M. Watanabe, D. Wilson, J. Fujimoto, and A. Rollins: Ultrahigh-speed optical coherence tomography imaging and visualization of the embryonic avian heart using a buffered Fourier Domain Mode Locked laser. Opt Express, 15, 6251–6267 (2007) DOI: 10.1364/OE.15.006251
[19] F. Shi, X. Chen, H. Zhao, W. Zhu, D. Xiang, E. Gao, M. Sonka, and H. Chen: Automated 3-D Retinal Layer Segmentation of Macular Optical Coherence Tomography Images With Serous Pigment Epithelial Detachments. IEEE Trans Med Imaging, 34, 441–452 (2015) DOI: 10.1109/TMI.2014.2359980
[20] J. Sugmk, S. Kiattisin, and A. Leelasantitham: Automated classification between agerelated macular degeneration and Diabetic macular edema in OCT image using image segmentation. 7 th Biomedical Engineering International Conference (BMEiCON), 1–4 (2014) DOI: 10.1109/bmeicon.2014.7017441
[21] A. Lang, A. Carass, B. M. Jedynak, S. D. Solomon, P. A. Calabresi, and J. L. Prince: Intensity inhomogeneity correction of macular OCT using N3 and retinal flatspace. IEEE 13th International Symposium on Biomedical Imaging (ISBI), 197–200 (2016) DOI: 10.1109/isbi.2016.7493243
[22] Wali, Asad, and Arjun Sipani. "Effects of Filters in Retinal Disease Detection on Optical Coherence Tomography (OCT) Images Using Machine Learning Classifiers." vol. 6, pp. 83-97, 2024.
[23] P. P. Srinivasan et al., "Fully automated detection of diabetic macular edema and dry age-related macular d egeneration from optical coherence tomography images", Biomed. Opt. Exp., vol. 5, pp. 3568-3577, 2014.
[24] Schmidt-Erfurth, et al, “Unsupervised identification of disease marker candidates in retinal oct imaging data,” IEEE transactions on medical imaging, vol. 38, pp. 1037–1047, 2019.
[25] Lee C.S., Baughman D.M., Lee A.Y. Deep Learning Is Effective for Classifying Normal versus Age-Related Macular Degeneration OCT Images. Ophthalmol. Retin. 2017;1:322–327. doi: 10.1016/j.oret.2016.12.009.
[26] Kermany DS, Goldbaum M, Cai W, Lewis MA. Identifying Medical Diagnoses and Treatable Diseases by Image-Based Deep Learning Resource Identifying Medical Diagnoses and Treatable Diseases by Image-Based Deep Learning. Cell. 2018;172:1122–31.e9. https://doi.org/10.1016/j.cell.2018.02.010.
[27] Huang L., He X., Fang L., Rabbani H., Chen X. Automatic Classification of Retinal Optical Coherence Tomography Images With Layer Guided Convolutional Neural Network. IEEE Signal Process. Lett. 2019;26:1026–1030. doi: 10.1109/LSP.2019.2917779.
[28] Chowdhary C.L., Acharjya D. Clustering Algorithm in Possibilistic Exponential Fuzzy C-Mean Segmenting Medical Images. J. Biomimetics Biomater. Biomed. Eng. 2017;30:12–23. doi: 10.4028/www.scientific.net/JBBBE.30.12.
[29] T. Tsuji et al., “Classification of optical coherence tomography images using a

capsule network," BMC Ophthalmol., vol. 20, no. 1, pp. 1–9, Mar. 2020, doi: 10.1186/S12886-020-01382-4/FIGURES/9.

[30] G. Latha and P. Aruna Priya, "Glaucoma Retinal Image Detection and Classification using Machine Learning Algorithms," J. Phys. Conf. Ser., vol. 2335, no. 1, p. 012025, Sep. 2022, doi: 10.1088/1742-6596/2335/1/012025.

[31] S. Roychowdhury, D. D. Koozekanani, S. Radwan, and K. K. Parhi: Automated localization of cysts in diabetic macular edema using optical coherence tomography images. 35th Annual International Conference of the IEEE Engineering in Medicine and Biology Society (EMBC), 1426–1429 (2013) DOI: 10.1109/embc.2013.6609778

[32] Y. Zhou, "Automated Identification of Diabetic Retinopathy Using Deep Learning," 2021.

[33] Jian Li, "Automated Detection and Classification of Diabetic Retinopathy Using Deep Learning Based on EfficientNet," 2020

[34] H. Fu, "Automated diagnosis of diabetic retinopathy using deep learning", 2018

[35] S. W. Ting et al., "Artificial intelligence and deep learning in ophthalmology," Br. J. Ophthalmol., vol. 103, no. 2, pp. 167–175, Feb. 2019, doi: 10.1136/BJOPHTHALMOL-2018- 313173.

[36] R. Gargeya and T. Leng, "Automated Identification of Diabetic Retinopathy Using Deep Learning," Ophthalmology, vol. 124, no. 7, pp. 962–969, Jul. 2017, doi: 10.1016/J.OPHTHA.2017.02.008.

[37] Hwang D.K., Hsu C.C., Chang K.J., Chao D., Sun C.H., Jheng Y.C., Yarmishyn A.A., Wu J.C., Tsai C.Y., Wang M.L., et al. Artificial intelligence-based decision-making for age-related macular degeneration. Theranostics. 2019;9:232–245. doi: 10.7150/thno.28447.

[38] Tasnim N., Hasan M., Islam I. Comparisonal study of Deep Learning approaches on Retinal OCT Image. arXiv. 20191912.07783